Journal of Medicinal Chemistry

ARTICLE

pubs.acs.org/jmc

Synthesis of Three Novel Fluorine-18 Labeled Analogues of L-Deprenyl for Positron Emission Tomography (PET) studies of Monoamine Oxidase B (MAO-B)

Sangram Nag,*[,†] Lutz Lehmann,[‡] Tobias Heinrich,[‡] Andrea Thiele,[‡] Georg Kettschau,[‡] Ryuji Nakao,[†] Balázs Gulyás,[†] and Christer Halldin[†]

[†]Karolinska Institutet, Department of Clinical Neuroscience, Psychiatry Section, Karolinska Hospital, S-17176 Stockholm, Sweden

[‡]Bayer Healthcare AG, Global Drug Discovery, Berlin, Germany

Supporting Information

ABSTRACT: The aim in this project was to synthesize and to study fluorine-18 labeled analogues of L-deprenyl which bind selectively to the enzyme monoamine oxidase B (MAO-B). Three fluorinated L-deprenyl analogues have been generated in multistep organic syntheses. The most promising fluorine-18 compound *N*-[-(2*S*)-1-[^{18}F]fluoro-3-phenylpropan-2-yl]-*N*-methylprop-2-yn-1-amine (**4c**) was synthesized by a one-step fluorine-18 nucleophilic substitution reaction. Autoradiography on human brain tissue sections demonstrated specific binding for compound **4c** to brain regions known to have a high content of MAO-B. In addition, the corresponding nonradioactive fluorine-19 compound (**13**) inhibited recombinant human MAO-B with an IC_{50} of 170.5 ± 29 nM but did not inhibit recombinant human MAO-A (IC_{50} > 2000 nM), demonstrating its specificity. Biodistribution of **4c** in mice showed high initial brain uptake leveling at 5.2 ± 0.04%ID/g after 2 min post injection. In conclusion, compound **4c** is a specific inhibitor of MAO-B with high initial brain uptake in mice and is, therefore, a candidate for further investigation in PET.

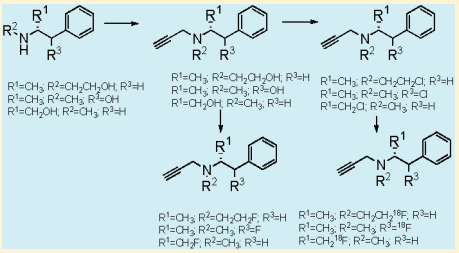

INTRODUCTION

Monoamine oxidases (MAO) are important enzymes regulating the levels of monoaminergic neurotransmitters and of bioactive monoamines by catalyzing their deamination.[1] Biochemical and pharmacological studies indicate that the MAO enzyme exists in two isoforms known as "MAO type A" (MAO-A) and "MAO type B" (MAO-B).[2] The isoforms differ in their distribution in body organs and in their substrate specificity. In general, MAO-A selectively oxidizes the "neurotransmitter" monoamines such as epinephrine, norepinephrine, and 5-hydroxytryptamine, while MAO-B selectively oxidizes the monoamines such as *O*-tyramine, phenethylamine and tele-*N*-methyl histamine and both MAO-A and MAO-B isoforms generate hydrogen peroxide which can form highly reactive oxygen species. Both MAO-A and MAO-B oxidize tyramine, tryptamine, and dopamine.[3] The MAO isoforms also differ according to their inhibition selectivity and thus can be inhibited depending upon the chemical structure of the inhibitor or the relative concentrations of the inhibitor and the enzyme. MAO inhibitors are used for the treatment of psychiatric and neurological disorders. MAO-A inhibitors are prescribed mainly for depression,[4] and MAO-B inhibitors are mostly used to treat Parkinson's disease (PD)[5] as well as depression.[6,7] MAO-A is selectively inhibited by, e.g. pirlindole and clorgyline, whereas MAO-B is selectively inhibited by e.g. L-deprenyl and rasagiline (Figure 1).

In the human brain, the presence of MAO-B predominates over MAO-A and constitutes up to ∼70% of total brain MAO activity.[8] Cerebral MAO-B levels increase with age and are further up-regulated in the brains of AD patients, mostly due to an increase of reactive astrocytes.[9] As astrocyte activity and, consequently, the activity of the MAO-B system, is up-regulated in neuroinflammatory processes, radiolabeled MAO-B inhibitors may serve as an imaging biomarker in neuroinflammation and neurodegeneration, including Alzheimer's disease.[10,11]

Positron emission tomography (PET), a high-resolution, sensitive, and noninvasive imaging technique, has been widely utilized in visualizing the localization of MAO-B. Imaging brain MAO-B activity with PET in humans has been useful for studying neurodegenerative diseases[12,13] and epilepsy.[14] Carbon-11 labeled L-deprenyl was demonstrated as useful tracer for assessing MAO-B.[15−17] The short half-life of carbon-11 (20.4 min) makes these tracers less suitable for distribution to PET centers not equipped with an on-site cyclotron. Therefore, there has been much interest in the development of labeled MAO inhibitors with longer half-life as biological probes to map MAO activity. A fluorine-18 labeled MAO-B inhibitor would offer a longer half-life of 110 min, but so far no successful PET radioligand has been fully validated. Clorgyline was previously labeled with fluorine-18 at aromatic and aliphatic positions, and the resulting tracers were shown to have favorable properties for mapping MAO-A activity

Received: March 22, 2011
Published: September 19, 2011

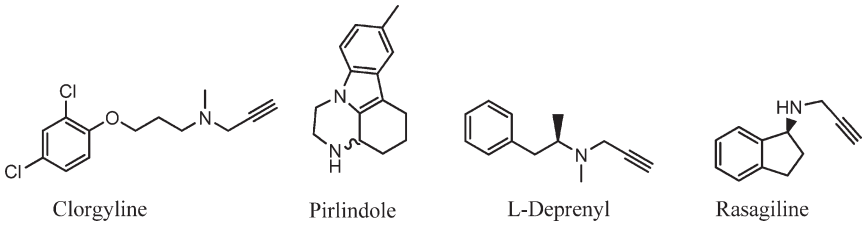

Figure 1. Structures of common MAO inhibitors.

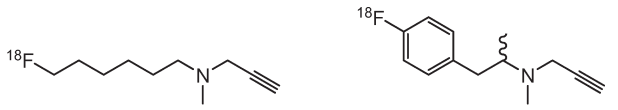

Figure 2. Structures of two [^{18}F]labeled MAO-B inhibitors.

in the brain.[18] Two fluorine-18 labeled MAO-B PET radioligands (Figure 2), 6-[^{18}F]fluoro-*N*-methyl-*N*-(prop-2-yn-1-yl)hexan-1-amine[19] and DL-4-[^{18}F]fluorodeprenyl[20] were synthesized for mapping MAO-B activity. The 6-[^{18}F]fluoro-*N*-methyl-*N*-(prop-2-yn-1-yl)hexan-1-amine has not been fully validated for clinical study, and the multistep radiosynthesis of DL-4-[^{18}F]fluorodeprenyl precludes its routine synthesis.

In this project, our aims were (i) to develop a fast and efficient synthetic method for labeling novel L-deprenyl analogues with fluorine-18 at the aliphatic chain and (ii) to evaluate their binding to MAO-B in various brain structures in post mortem human brain slices using an autoradiography technique in order to select a suitable fluorine-18 labeled radioligand for in vivo molecular imaging studies using PET.

RESULTS AND DISCUSSION

Chemistry. Three novel fluorinated analogues of L-deprenyl **2**, **8**, and **13** (Scheme 1) were prepared. To label compounds **2**, **8**, and **13** with fluorine-18 to obtain **4a**, **4b**, and **4c**, respectively, three appropriate chloro-precursors **4**, **9**, and **15**, needed to be synthesized. The chloro precursor **4** for labeling with fluorine-18 was prepared according to Scheme 1. From commercially available **1** (desmethyl deprenyl hydrochloride salt), fluoride **2** and alcohol **3** were synthesized by alkylation of secondary amine using sodium hydroxide as strong base. In the next step, alcohol **3** was treated with mesyl chloride and instead of *N*-(2-mesylethyl)-*N*-(1-phenylpropan-2-yl)prop-2-yn-1-amine, *N*-(2-chloroethyl)-*N*-(1-phenylpropan-2-yl)prop-2-yn-1-amine (**4**) was produced. Initially the reaction was performed at −7 °C; however, the reaction did not proceed at that low temperature. Subsequently, the reaction temperature was allowed to increase slowly, and progress of the reaction was monitored by TLC. At 10 °C, the reaction commenced but went directly through to give chloride **4** by immediate substitution of the intermediate mesylate group by S_N2 substitution reaction with concomitant chloride formed in the initial mesylation reaction.

Amines **6** and **11** were prepared from commercially available carbamate **5** and amino acid **10** by reduction with $LiAlH_4$ following a previously described procedure.[21] Amino alcohols **6** and **11** were alkylated with propargyl bromide,[22] and the obtained alcohols **7** and **12** were chlorinated upon treatment with mesyl

Scheme 1. Synthesis of Precursor and Reference for 4a, 4b, and 4c[a]

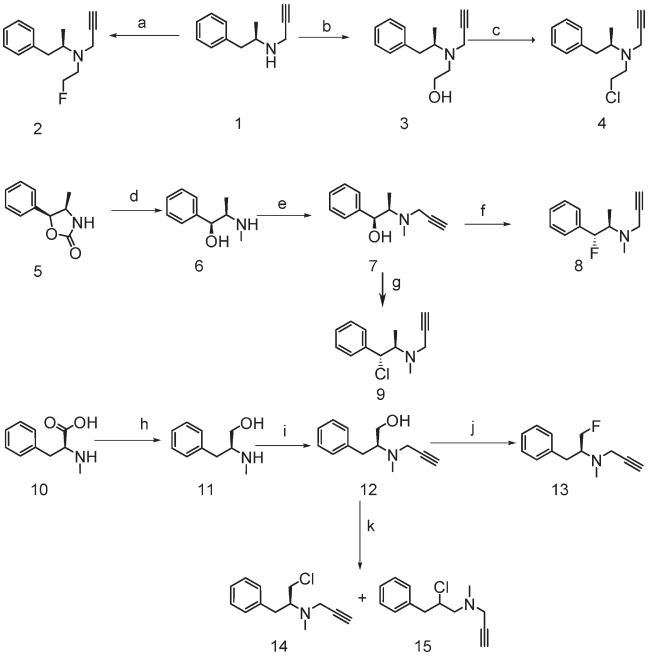

[a] Conditions: (a) NaOH/1-fluoro 2-bromo ethane; (b) NaOH/1-bromoethanol; (c) TEA/mesyl chloride; (d) LAH; (e) K_2CO_3/propargyl bromide; (f) DAST; (g) TEA/mesyl chloride; (h) LAH; (i) K_2CO_3/propargyl bromide; (j) DAST; (k) TEA/mesyl chloride.

chloride. A mixture of two chlorinated isomers **14** and **15** was formed from **12**. Fluorides **8** and **13** were synthesized from amino alcohols **7** and **12** by fluorination with diethylamino sulfurtrifluoride (DAST). The formation of chlorides **14** and **15** can be explained by an intermediate aziridinium ion **17** resulting from an intramolecular nucleophilic attack (S_Ni) of the free electron pair of the nitrogen.[23]

Chlorides **14** and **15** were then formed by subsequent nucleophilic attack (S_N2) of Cl^- at the corresponding reactive position of aziridinium ion **17** (Scheme 2). Compounds **14** and **15** were formed in a molar ratio of 2:1 in the isomeric mixture as indicated by the *N*-Me ^{1}H NMR signals.

Radiochemistry. The radiolabeling was achieved by one-step nucleophilic substitution reactions of the chloride precursors (**4**, **9**, and mixture of **14** and **15**) by [^{18}F]fluoride in presence of $K_{2.2.2}$ and K_2CO_3 as shown in Scheme 3. Azeotropic drying was performed before the dried K[^{18}F]F$^-$$K_{2.2.2}$ complex was treated with the adequate chloride precursor in anhydrous DMSO. The reaction mixtures were heated at 120 °C for 20 min to form the respective fluorine-18 labeled

dx.doi.org/10.1021/jm200710b |*J. Med. Chem.* 2011, 54, 7023–7029

product. Compound **4c** was purified from the isomeric mixture of **4c** and **4d** by HPLC. The overall radiosynthesis, including fluorination, HPLC purification, and evaporation of the solvent and radiotracer formulation, was completed in a time range of 70−80 min.

The incorporation yield of the fluorination reactions varied from 40% to 70%, and the radiochemical purity was greater than 99% for fluorine-18 labeled **4a**, **4b**, and **4c** throughout (Table 1). The identities of the labeled compounds were confirmed by coinjection of their corresponding fluorine-19 analogues **2**, **8**, and **13** using analytical HPLC. All radioligands were found to be stable in PBS buffered solution (pH = 7.4) for the duration of 180 min with a half-life of 110 min.

In Vitro Inhibition of MAO-A and MAO-B. IC_{50} values for inhibition of MAO-B and MAO-A were determined based on the rate of kynuramine oxidation for the analogues of L-deprenyl in order to determine their specificity for binding to MAO-B. Compounds **2** and **8** inhibited MAO-B with an IC_{50} greater than 2 μM and were therefore not further investigated for their specificity toward MAO-A. Compound **13** featured an IC_{50} of 170.5 ± 29 nM for its MAO-B inhibitory activity while it was not inhibiting MAO-A (IC_{50} > 2 μM). L-Deprenyl was used as reference compound. It inhibited MAO-B with an IC_{50} of 85.2 ± 26.9 nM. Thus, compound **13** inhibited MAO-B in a range comparable to that of the therapeutically used compound. Clorgyline inhibited MAO-A with an IC_{50} of 30.2 ± 11.5 nM.

Autoradiography. All three novel MAO-B fluorine-18 fluorodeprenyl analogues, **4a**, **4b**, and **4c**, were tested in human whole hemisphere autoradiography experiments on brain tissue, obtained from deceased subjects with no sign of any brain disorders. First, **4a** featured only a moderate binding to the white matter and no binding to the cortical gray matter. The white matter binding could not be blocked with the cold ligand, L-deprenyl itself, or with the specific MAO-A and MAO-B ligands pirlindole and rasagiline, respectively, indicating that the observed binding is mainly nonspecific. Using **4b**, there a low level binding to the cortex was found, with the highest but still moderate binding affinity to the hippocampus at baseline condition. Blocking with L-deprenyl and rasagiline both abolished the binding, whereas pirlindole did not block the binding, indicating that **4b** displays a weak but specific binding to MAO-B rich cortical structures (data not shown).

Compound **4c** demonstrated total binding patterns, i.e. binding comprising specific and nonspecific binding within brain slices of AD brains and age matched controls. The baseline condition (total binding) is shown in panel A (Figure 3). For blocking, the MAO-B ligands L-deprenyl (panel B) and rasagiline (panel C), the MAO-A ligand pirlindole (panel D) have been used in 10 μM concentrations (Figure 3). Using the MAO-B ligands rasagiline and L-deprenyl, the binding of **4c** was completely blocked, whereas the MAO-A ligand pirlindole did not block the total binding. This indicates that **4c** is a selective radioligand of the MAO-B isoform, whereas it displays no binding to MAO-A. Compared with **4a** and **4b**, the binding of **4c** in all brain structures was higher. The signal intensities were highest in the hippocampus, the perihippocampal gyrus, the temporal lobe, and to some extent, the parietal lobe. There was also increased signal intensity in the white matter adjacent to layer 6 of the cortex.

Plasma Protein Binding. Plasma protein binding was measured using an ultrafiltration method. The results were corrected for the membrane binding as measured with the control samples. Binding of **4c** to monkey and human plasma proteins were 75.9 ± 0.1% and 83.2 ± 0.5%, respectively. Therefore, there was a measurable free fraction of **4c** in plasma: 24.1 ± 0.1% and 16.8 ± 0.5% for monkey and human, respectively.

Biodistribution. The biodistribution of compound **4c** was investigated in NMRI mice at five time points, namely 2, 5, 30, 60, and 240 min, and showed a high initial brain uptake of radioactivity leveling at 5.2 ± 0.04%ID/g at 2 min post injection. In addition, a high initial elimination of radioactivity from the brain was observed, reaching a level of 1.9 ± 0.33% ID/g at 30 min pi and decreased further to 1.4 ± 0.26% ID/g at the 4 h time point pi. The initial brain uptake was higher as the measured blood value. This is shown in Figure 4. In addition, the biodistribution result of **4c** in NMRI mice differs to the literature data for [^{11}C]deprenyl brain kinetics in mice.[16] For [^{11}C]deprenyl, the brain over blood ratio increased with time whereas for compound **4c** a decrease of this ratio had been observed. A probable explanation behind this observation is that compound **4c** (fluorodeprenyl) is a different compound as compared to deprenyl, and for that reason its behavior in biodistribution experiments in mice could differ from the data observed with [^{11}C]deprenyl. Another reason for the differences could be the use of another mouse strain that could lead to different results.

Scheme 2. Proposed Mechanism for the Formation of 14 and 15

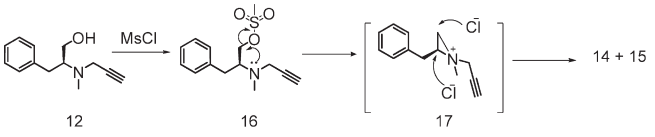

Scheme 3. Radiolabeling of 4a, 4b, and 4c

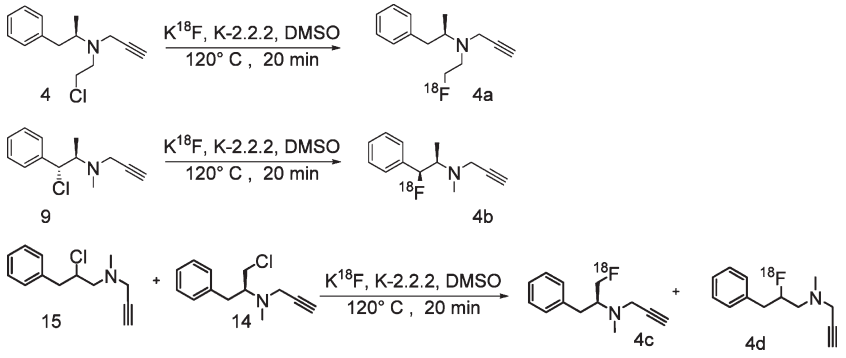

Table 1. Result of Radiochemistry

radioligand	total synthesis time (min)	radiochemical yield (%)	radiochemical purity (%)	preparative HPLC retention time (min)	analytical HPLC retention time (min)	specific radioactivity (GBq/μmol)	TLC-Rf
4a	70−80	41 (N = 6)	>99	11−13	5.3	240	0.68
4b	70−80	46 (N = 2)	>99	9−11	5.4	310	0.63
4c	70−80	68 (N = 3)	>99	14−16	6.7	280	0.60

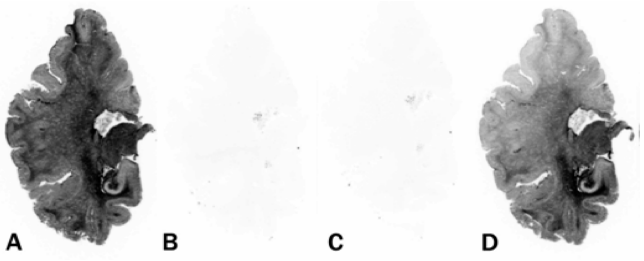

Figure 3. Coronal slices of human brain autoradiograms labeled with **4c**. (A) Baseline conditions. (B) Incubation with L-deprenyl (10 μM). (C) Incubation with rasagiline (10 μM). (D) Incubation with pirlindole (10 μM). The brain slices were obtained from a 58 y old female control subject; the post mortem time was 11 h.

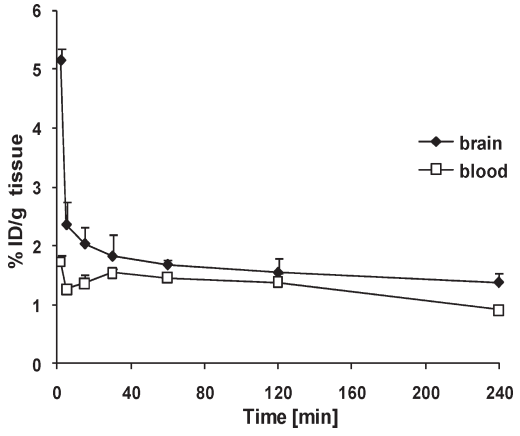

Figure 4. Time course distribution of compound **4c** in brain and blood of male NMRI mice.

CONCLUSION

Radiolabeling of three new fluorine-18 analogues of L-deprenyl was successfully accomplished with adequate radiochemical yields, high specific radioactivity, and radiochemical purity higher than 99%. Biodistribution in mice showed that compound **4c** adequately passed the blood−brain barrier. The fluorine-18 labeled compound **4c** binds specifically to MAO B in post mortem human brain sections. Consequently, radioligand **4c** appears to be a potential molecular imaging biomarker candidate for PET studies in neuroinflammation and neurodegeneration, accompanied with astrocyte activation.

EXPERIMENTAL SECTION

Chemistry. NMR spectra were recorded on Varian Unity-400 and Bruker Avance 400 (^{1}H, 400 MHz; ^{13}C, 100 MHz) and Bruker Avance 600 III (^{1}H, 600 MHz) NMR instruments. ^{1}H NMR spectra were referenced internally on $CDCl_3$ (δ^1H 7.26) and ^{13}C NMR spectra were referenced internally on $CDCl_3$ (δ^{13}C 77.20). Liquid chromatographic analysis (LC) was performed with a Merck−Hitachi gradient pump and a Merck−Hitachi L-4000 variable wavelength UV-detector. A μ-Bondapak C-18 column (300 mm × 7.8 mm, 10 μm; Waters instruments) was used with a flow of 2 mL/min. LC-MS was performed using a Waters Quattra-Tof Premier micro mass spectrometer or Waters SQD 3001 single quadrupole mass spectrometer, coupled to Waters Acquity UPLC instruments. The ionization mode used was electro spray positive ionization (ESI+). Analytical TLC was carried out on 0.25 mm silica gel plates.

All solvents and chemicals were obtained from commercial sources and used without further purification. Purity of all compounds is ≥95% and was determined by HPLC and UPLC and LC-MS.

*Synthesis of N-(2-Chloroethyl)-N-[(2R)-1-phenylpropan-2-yl]prop-2-yn-1-amine (**4**).* A mixture of **3** (150 mg, 0.69 mmol) and triethyl amine (1.5 mmol) in THF (3 mL) was stirred at room temperature for 30 min. To the stirred mixture mesyl chloride (1.4 mmol) was added dropwise at −7 °C, and the reaction mixture was stirred at 10 °C for additional 30 min. Saturated Na_2CO_3 solution (2 mL) was added and stirred for 30 more min. The organic layer was partitioned between CH_2Cl_2 (20 mL) and water (10 mL). The organic phase was separated and washed with saturated $NaHCO_3$ solution (10 mL) and brine (10 mL) and dried over $MgSO_4$ and filtered. The solvent was removed under reduced pressure to obtain the crude product as light-yellow oil. The crude product was purified by silica-gel column chromatography (hexane/ether 3:1), and the final product resulted as colorless oil (85 mg, 0.63 mmol, 52%). The product was analyzed by NMR and LC-MS.

^{1}H NMR (^{1}H, 400 MHz, $CDCl_3$) δ_H: 1.0 (3H, d), 2.2 (1H, s), 2.4 (1H, m), 2.9−3.1 (4H, m), 3.4−3.6 (4H, m), 7.1−7.4 (5H, m).

^{13}C NMR (^{13}C, 100 MHz, $CDCl_3$) δ_C: 16.1, 40.1, 40.6, 42.6, 51.6, 59.9, 71.1, 126.0, 127.6, 129.2, 140.0.

LC-MS (ESI): m/z = 236 (M + 1).

*Synthesis of N-((1R,2S)-1-Fluoro-1-phenylpropan-2-yl)-N-methylprop-2-yn-1-amine (**8**).* To the stirred solution of **7** (150 mg, 0.74 mmol) in dichloromethane (3 mL), diethylamino sulfurtrifluoride (DAST) (1.0 mmol) was added dropwise at −5 °C and the reaction mixture was stirred for additional 20 min at the same temperature. Saturated aqueous sodium carbonate (2.0 mL) was added to quench unreacted DAST. The organic layer was partitioned between CH_2Cl_2 (15 mL) and water (10 mL). The organic phase was separated and washed with brine (10 mL) and dried over $MgSO_4$ and filtered. The solvent was removed under reduced pressure to obtain the crude product as light-yellow oil. The crude product was purified by silica-gel column chromatography (hexane/ether 4:1). Final product was obtained as light-yellow oil (75 mg, 0.37 mmol, 49%) and was analyzed by NMR, HPLC and LC-MS.

^{1}H NMR (^{1}H, 400 MHz, $CDCl_3$) δ_H: 1.1 (3H, d), 2.3 (1H, s), 2.4 (3H, s), 3.1−3.2 (1H, m), 3.5 (2H, s), 5.7 (1H, d) and 7.3−7.5 (5H, m).

^{13}C NMR (^{13}C, 100 MHz, $CDCl_3$) δ_C: 8.4, 39.6, 43.8, 62.5, 73.5, 93.5, 95.2, 125.5, 128.1, 129.9 and 141.5.

LC-MS (ESI): m/z = 206 (M + 1).

*Synthesis of N-((1R,2S)-1-Chloro-1-phenylpropan-2-yl)-N-methylprop-2-yn-1-amine (**9**).* A mixture of **7** (120 mg, 0.54 mmol) and triethyl amine (88 μL, 1.0 mmol) in THF (2 mL) was stirred at room temperature for 30 min. To the stirred mixture mesyl chloride (46.44 μL,

0.60 mmol) was added dropwise at −7 °C, and the reaction mixture was stirred at room temperature for additional 30 min. Saturated Na_2CO_3 solution (1 mL) was added and stirred for additional 30 min. The organic layer was partitioned between CH_2Cl_2 (15 mL) and water (10 mL). The organic phase was separated and washed with saturated $NaHCO_3$ solution (10 mL) and brine (10 mL) and dried over $MgSO_4$ and filtered. The solvent was removed under reduced pressure to obtain the crude product as light-yellow oil. The crude product was purified by silica-gel column chromatography (hexane/ether 3:1). Final product was obtained as a light-yellow oil (91 mg, 0.41 mmol, 69%) and was analyzed by NMR, HPLC, and LC-MS.

^{1}H NMR. (^{1}H, 400 MHz, $CDCl_3$) δ_H: 1.3 (3H, d), 2.3 (1H, s), 2.4 (3H, s), 3.2−3.3 (1H, m), 3.5 (2H, s), 4.5 (1H, d) and 7.2−7.4 (5H, m).

^{13}C NMR (^{13}C, 100 MHz, $CDCl_3$) δ_C: 22.9, 31.6, 39.7, 43.9, 57.1, 71.4, 73.8, 127.5, 128.1, 129.9 and 136.1.

LC-MS (ESI): m/z = 222 (M + 1).

*Synthesis of (S)-N-(1-Fluoro-3-phenylpropan-2-yl)-N-methylprop-2-yn-1-amine (**13**).* To the stirred solution of **12** (300 mg, 1.48 mmol) in dichloromethane (5 mL), diethylamino sulfurtrifluoride (264 μL, 2.0 mmol) was added dropwise at −5 °C and the reaction mixture was stirred for additional 20 min at the same temperature. Saturated sodium carbonate (4.0 mL) was added to quench unreacted DAST. The organic layer was partitioned between CH_2Cl_2 (25 mL) and water (15 mL). The organic phase was separated and washed with brine (10 mL) and dried over $MgSO_4$ and filtered. The solvent was removed under reduced pressure to obtain the crude product as a light-yellow oil. The crude product was purified by silica-gel column chromatography (hexane/ether 3:1) and gave the final product (65 mg, 0.32 mmol, 21%). The product was analyzed by NMR, HPLC, and LC-MS.

^{1}H NMR (600 MHz, chloroform-*d*) δ ppm: 2.3 (t, 1 H), 2.55 (s, 3 H), 2.77 (dd, 1 H), 2.97−3.03 (m, 1 H), 3.03−3.14 (m, 1 H), 3.53 (t, 2 H), 4.38 (ddd, 1 H), 4.51 (ddd, J = 48.05, 10.27, 2.57 Hz, 1 H), 7.20−7.32 (m, 5H).

^{13}C NMR (151 MHz, $CDCl_3$) δ ppm 39.7, 42.4, 46.3, 58.5, 73.4, 78.2, 92.8, 126.6, 128.4, 129.4 and 136.8.

LC-MS (ESI): m/z = 206 (M + 1).

*Synthesis of (S)-N-(1-Chloro-3-phenylpropan-2-yl)-N-methylprop-2-yn-1-amine (**14**) and N-(2-Chloro-3-phenylpropyl)-N-methylprop-2-yn-1-amine (**15**).* A mixture of **12** (100 mg, 0.49 mmol) and triethyl amine (139 μL, 1.0 mmol) in THF (2 mL) was stirred at room temperature for 30 min. To the stirred mixture mesyl chloride (68.7 mg, 46.4 μL, 0.60 mmol) was added dropwise at −7 °C, and the reaction mixture was stirred at room temperature for additional 30 min. Saturated aqueous Na_2CO_3 solution (1 mL) was added and stirred for further 30 min. The organic layer was partitioned between CH_2Cl_2 (15 mL) and water (10 mL). The organic phase was separated and washed with saturated $NaHCO_3$ solution (10 mL) and brine (10 mL), dried over $MgSO_4$, and filtered. The solvent was removed under reduced pressure to obtain the crude product as a light-yellow oil. The crude product was purified by silica-gel column chromatography (hexane/ether 3:1) and final product (90 mg, 82%, 0.41 mmol) was obtained as a light-yellow oil. The product was analyzed by NMR, HPLC, and LC-MS. The final product was a mixture of **14** (major) and **15** (minor).

14 (major): ^{1}H NMR (^{1}H, 400 MHz, $CDCl_3$) δ_H 2.28 (t, 1 H), 2.51 (s, 3 H), 2.78 (d, 2 H), 3.06 (dd, 1 H), 3.50 (dd, 2 H), 3.55−3.65 (m, 2 H), 7.30−7.41 (m, 5 H).

LC-MS (ESI): m/z = 222 (M + 1).

15 (minor): ^{1}H NMR (^{1}H, 400 MHz, $CDCl_3$) δ_H 2.21 (t, 1 H), 2.38 (s, 3 H), 2.74 (d, 2 H), 2.94 (dd, J = 14.22, 1 H), 3.23 (dd, 1 H), 3.43 (t, 2 H), 4.08−4.20 (m, 1 H), 7.22−7.26 (m, 2 H), 7.26−7.36 (m, 3 H).

LC-MS (ESI): m/z = 222 (M + 1).

Radiochemistry. *Synthesis of N-[2-[^{18}F]Fluoroethyl]-N-[(2R)-1-phenylpropan-2-yl]prop-2-yn-1-amine (**4a**), N-[(1S,2R)-1-[^{18}F]Fluoro-1-phenylpropan-2-yl]-N-methylprop-2-yn-1-amine (**4b**), and N-[(2S)-1-[^{18}F]Fluoro-3-phenylpropan-2-yl]-N-methylprop-2-yn-1-amine (**4c**).* Fluorine-18 fluoride was produced by the ^{18}O(p, n)^{18}F nuclear reaction using a GEMS PETtrace cyclotron. A solution of [^{18}F]fluoride in ^{18}O enriched water was flashed through a Sep-Pak QMA light cartridge (preconditioned with K_2CO_3 (0.5 M, 10 mL), 18 MΩ H_2O, 15 mL) in order to isolate [^{18}F]fluoride. [^{18}F]Fluoride was then eluted from the cartridge with a solution of K_2CO_3 (1.8 mg, 13 μmol), Kryptofix 2.2.2 (9.8 mg, 26 μmol) in water (18 MΩ, 43 μL), and acetonitrile (2 mL). The solvent was evaporated at 160 °C under continuous nitrogen flow. The residue was then cooled to 25 °C, followed by addition of the precursor **4**, **9**, or **15** (2.0 mg, ∼0.01 mmol, in DMSO (600 μL)) was added. The closed reaction vessel was then heated at 120 °C for 20 min. The reaction vessel was cooled to room temperature, and 18 MΩ H_2O (1 mL) was added before injecting to the HPLC.

All three fluorine-18 labeled radioligands **4a**, **4b**, and **4c** were purified by reverse phase HPLC on a μ-Bondapak C-18 column (300 mm × 7.8 mm, 10 μm; waters instruments) and MeCN−H_3PO_4 (0.01 M) (15:85 v/v) was used as the eluting solvent at a flow rate of 4 mL/min. Elute was monitored by a UV absorbance detector (λ = 214 nm) in series with a GM tube radioactivity detector. The isomeric mixture of **4c** and **4d** was separated by HPLC ($t_{R(4c)}$ = 14−16 min, $t_{R(4d)}$ = 18−19 min). The fraction of the desired compounds was collected and evaporated to dryness. The residue was dissolved in sterile disodiumphosphate phosphate buffered saline (PBS; pH = 7.4; 10 mL) and filtered through a sterile filter (0.22 μm; Millipore, Bedford, MA), yielding a sterile and pyrogen-free (<1.25 EU) solution of the radioligand.

The radiochemical purity of each radioligand (**4a**, **4b**, and **4c**) was analyzed by a reverse phase HPLC on a μ-Bondapak C-18 column (300 mm × 3.9 mm, 10 μm; waters instruments) and MeCN−H_3PO_4 (0.01 M) (15:85 v/v) was used as the eluting solvent at a flow rate of 2 mL/min. Elute was monitored by a UV absorbance detector (λ = 214 nm) in series with a radioactivity detector (β-flow; Beckman, Fullerton, CA). The radiochemical purity was >99% for all three compounds.

The stability and radiochemical yield was tested with HPLC and TLC on silica gel (100% $CH_3COOC_2H_5$ was used as the eluting solvent). TLC plate was scanned with an AR-2000 imaging scanner and analyzed with Winscan 2.2 software.

Determination of MAO Inhibition. Human recombinant MAO-B and MAO-A enzymes (Sigma) prepared from insect cells were purchased from Sigma. The assays were designed to determine the inhibition of kynuramine oxidation in the presence of the compounds of interest according to Weissbach et al.[24] A calibration curve of kynuramine hydrobromide (Sigma) was determined at 360 nm and used for calculation of the enzyme activity (pmol/min) at the respective compound concentration. This relation was plotted and the IC_{50} determined using the software GraFit 5 (Version 5.0.6). The assays were performed as follows. The compounds were diluted 1:2 in each step in 50 mM phosphate buffer (pH 7.4) so that a concentration curve between 0.49 and 1000 nM was generated to determine the IC_{50} for MAO-B and between 0.98 and 2000 nM for determination of inhibition of MAO-A, respectively. Kynuramine hydrobromide at a concentration of 125 μM for MAO-B and 100 μM for MAO-A, respectively, and 2.5 U/mL enzyme were added and the reaction followed measuring the absorption at 360 nm in a 5 min interval over 30 min at 37 °C. The 30 min time point was used to determine IC_{50} values. As internal standards for MAO-B, pargyline and L-deprenyl and for MAO-A clorgyline were used.

In Vitro Autoradiography. Human brains without pathology were obtained from the Department of Forensic and Insurance Medicine, Semmelweis University, Budapest. The brains had been removed during forensic autopsy (control brains) and were handled in a manner similar to that described previously.[25−27] Ethical permissions were obtained from the relevant Research Ethics Committee of the respective institutions. The sectioning of the brains and the autoradiography experiments were performed at the Department of Neuroscience, Karolinska Institutet. The sectioning took place on a Leica cryomacrocut

system. The resulting slices were horizontal brain slices of 100 μm thickness. The brain slices were obtained from a 58-year-old female control subject; the post mortem time was 11 h, until which the cadaver was stored at ±0 °C. After the removal of the brain, it was kept at −85 °C until sectioning. The whole hemisphere brain slices were kept at −25 °C until the autoradiographic procedures.

The autoradiographic procedures were basically identical with those used by us in former studies.[28] Briefly, 100 μm thick whole hemisphere sections were incubated for 90 min at room temperature with 4 MBq/200 mL of the corresponding radiotracer in 50 mM TRIS buffer pH 7.4 containing sodium chloride (120 mM), potassium chloride (5 mM), calcium chloride (2 mM), and albumin (0.1% w/v). After the incubation, the sections were washed in the same buffer three times for 5 min each time at room temperature, briefly dipped in ice-cold distilled water, dried, and exposed to phosphorimaging plates. The readings were made in a Fujifilm BAS-500 phosphorimager and digitized using a Fujifilm IP Eraser 3. Standards were prepared by serial dilution of the radioligand stock solution in assay buffer.

Blocking experiments were performed with 10 μM L-deprenyl, rasagiline, and pirlindol for fluorine-18 labeled deprenyl analogues **4a** and **4b**. For compound **4c**, blocking experiments were done with L-deprenyl, rasagiline, and pirlindol.

Biodistribution. Biodistribution was investigated in male NMRI mice at five time points, namely 2, 5, 30, 60, and 240 min. The mice used in the experiments weighted between 25.0 and 31.5 g. For each time point, three mice were examined. The mice were injected each with 0.178 MBq radioactively labeled deprenyl analogues dissolved in 0.9% NaCl solution. At the respective post-injection time points, the mice were euthanized with an overdose of isofluorane, sacrificed, the organs excised, and blood taken, respectively, before measuring the organ and blood radioactivity levels in a γ counter. In addition, faeces and urine were collected and measured in a γ counter, as well. The results were decay corrected and normalized to 1 g of tissue and to whole blood volume, respectively, and expressed as percent injected dose per gram tissue and blood (%ID/g), respectively.

Plasma Protein Binding. Plasma protein binding of **4c** was measured in duplicate in baseline conditions. Monkey plasma (500 μL), human plasma (500 μL), and phosphate buffered saline solution (pH 7.4, KCl 0.2 mg, KH_2PO_4 0.2 mg, Na_2HPO_4 1.42 mg, NaCl 8 mg in 1 mL) serving as control, respectively, were mixed with **4c** radiopharmaceutical formulation (50 μL, approximately 20 MBq in PBS) and incubated at room temperature for 10 min. Samples (20 μL) from each incubation mixture were measured in a well-counter. After incubation, 200 μL portions of the incubation mixtures were pipetted into ultrafiltration tubes (Millipore Centrifree YM-30) and centrifuged for 15 min in 3000 rpm. Samples (20 μL) from each filtrate were counted in a well-counter. The fraction of protein-bound ligand was calculated using the following formula;

$$\frac{C_{\mathrm{pla(filtrate)}}}{C_{\mathrm{pla(total)}}} \div \frac{C_{\mathrm{PBS(filtrate)}}}{C_{\mathrm{PBS(total)}}} \times 100(\%)$$

where $C_{\mathrm{pla(total)}}$ and $C_{\mathrm{PBS(total)}}$ represent the radioactivity concentration of incubation mixture in plasma and PBS (control), respectively. $C_{\mathrm{pla(filtrate)}}$ and $C_{\mathrm{PBS(filtrate)}}$ are the radioactivity concentrations from filtrate samples.

■ ASSOCIATED CONTENT

Supporting Information. Experimental and spectroscopic details on compounds **2**, **3**, **6**, **7**, **11**, and **12**. This material is available free of charge via the Internet at http://pubs.acs.org.

■ AUTHOR INFORMATION

Corresponding Author

*Phone: +46-8-51775018. E-mail: sangram.nag@ki.se.

■ ACKNOWLEDGMENT

We thank all the members of the PET group at Karolinska Institutet, including special thanks to Siv Eriksson for excellent technical assistance with autoradiography. We also thank Bayer HealthCare AG for their support.

■ ABBREVIATIONS USED

PET, positron emission tomography; MAO, monoamino oxidase; PD, Parkinson's disease; AD, Alzheimer's disease; DAST, diethylamino sulfurtrifluoride; NMR, nuclear magnetic resonance; UPLC, ultra-performance liquid chromatograpy; DMSO, dimethylsuphoxide; DMF, dimethylformamide; PBS, phosphate buffer solution; IC, inhibitory concentration

■ REFERENCES

(1) Fuller, R. W.; Roush, B. W. Substrate-selective and tissue-selective inhibition of monoamine oxidase. *Arch. Int. Pharmacodyn. Ther.* **1972**, *198*, 270–276.

(2) Bach, A. W. J.; Lan, N. C.; Bruke, D. J.; Abell, C. W.; Bembenek, M. E.; Kwan, S. W.; Seeburg, P. H.; Shih, J. C. Molecular-cloning of human monoamine oxidase-A and oxidase-B (MAO-A and MAO-B). *FASEB J.* **1988**, *2*, A1733–A1733.

(3) Tipton, K. F.; Boyce, S.; O'Sullivan, J.; Davey, G. P.; Healy, J. Monoamine oxidases: certainties and uncertainties. *Curr. Med. Chem.* **2004**, *11*, 1965–1982.

(4) Andrews, J. M.; Nemeroff, C. B. Contemporary management of depression. *Am. J. Med.* **1994**, *97*, S24–S32.

(5) Drukarch, B.; van Muiswinkel, F. L. Drug treatment of Parkinson's disease—time for phase II. *Biochem. Pharmacol.* **2000**, *59*, 1023–1031.

(6) Youdim, M. B. H.; Bakhle, Y. S. Monoamine oxidase: isoforms and inhibitors in Parkinson's disease and depressive illness. *Br. J. Pharmacol.* **2006**, *147*, S287–S296.

(7) Holtzheimer, P. E.; Nemeroff, C. B. Emerging treatments for depression. *Expert Opin. Pharmacother.* **2006**, *7*, 2323–2339.

(8) Cesura, A. M.; Pletscher, A. The new generation of monoamine oxidase inhibitors. *Prog. Drug Res.* **1992**, *38*, 171–297.

(9) Saura, J.; Luque, J. M.; Cesura, A. M.; Da Prada, M.; Chan-Palay, V.; Huber, G.; Loffler, J.; Richards, J. G. Increased monoamine oxidase B activity in plaque-associated astrocytes of Alzheimer brains revealed by quantitative enzyme radioautography. *Neuroscience* **1994**, *62*, 15–30.

(10) Gulyas, B.; Pavlova, E.; Kasa, P.; Gulya, K.; Bakota, L.; Varszegi, S.; Keller, E.; Horvath, M. C.; Nag, S.; Hermecz, I.; Magyar, K.; Halldin, C. Activated MAO-B in the brain of Alzheimer patients, demonstrated by [(11)C]-l-deprenyl using whole hemisphere autoradiography. *Neurochem. Int.* **2011**, *58*, 60–68.

(11) Bench, C. J.; Price, G. W.; Lammertsma, A. A.; Cremer, J. C.; Luthra, S. K.; Turton, D.; Dolan, R. J.; Kettler, R.; Dingemanse, J.; Da Prada, M.; et al. Measurement of human cerebral monoamine oxidase type B (MAO-B) activity with positron emission tomography (PET): a dose ranging study with the reversible inhibitor Ro 19−6327. *Eur. J. Clin. Pharmacol.* **1991**, *40*, 169–173.

(12) Fowler, J. S.; Logan, J.; Volkow, N. D.; Wang, G. J.; MacGregor, R. R.; Ding, Y. S. Monoamine oxidase: radiotracer development and human studies. *Methods* **2002**, *27*, 263–277.

(13) Fowler, J. S.; Volkow, N. D.; Wang, G. J.; Pappas, N.; Shea, C.; MacGregor, R. R.; Logan, J. Visualization of monoamine oxidase in human brain. *Adv. Pharmacol.* **1998**, *42*, 304–307.

(14) Bergstrom, M.; Kumlien, E.; Lilja, A.; Tyrefors, N.; Westerberg, G.; Langstrom, B. Temporal lobe epilepsy visualized with PET with C-11-L-deuterium-deprenyl—analysis of kinetic data. *Acta Neurol. Scand.* **1998**, *98*, 224–231.

(15) Fowler, J. S.; MacGregor, R. R.; Wolf, A. P.; Arnett, C. D.; Dewey, S. L.; Schlyer, D.; Christman, D.; Logan, J.; Smith, M.; Sachs, H.; Aquilonius, S. M.; Bjurling, P.; Halldin, C.; Hartvig, P.; Leenders, K. L.; Lundqvist, H.; Oreland, L.; Stalnacke, C. G.; Langstrom, B. Mapping

human-brain monoamine oxidase-A and oxidase-B with C-11 labeled suicide inactivators and PET. *Science* **1987**, *235*, 481–485.

(16) MacGregor, R. R.; Halldin, C.; Fowler, J. S.; Wolf, A. P.; Arnett, C. D.; Langstrom, B.; Alexoff, D. Selective, irreversible in vivo binding of [11C]clorgyline and [11C]-L-deprenyl in mice: potential for measurement of functional monoamine oxidase activity in brain using positron emission tomography. *Biochem. Pharmacol.* **1985**, *34*, 3207–3210.

(17) Fowler, J. S.; Logan, J.; Wang, G. J.; Volkow, N. D.; Telang, F.; Ding, Y. S.; Shea, C.; Garza, V.; Xu, Y. W.; Li, Z. H.; Alexoff, D.; Vaska, P.; Ferrieri, R.; Schlyer, D.; Zhu, W.; Gatley, S. J. Comparison of the binding of the irreversible monoamine oxidase tracers, [C-11]clorgyline and [C-11]L-deprenyl in brain and peripheral organs in humans. *Nucl. Med. Biol.* **2004**, *31*, 313–319.

(18) Mukherjee, J.; Yang, Z. Y. Development of *N*-[3-(2′,4′-dichlorophenoxy)-2-F-18-fluoropropyl]-*N*-methylpropargylamine (F-18-fluoroclorgyline) as a potential PET radiotracer for monoamine oxidase-A. *Nucl. Med. Biol.* **1999**, *26*, 619–625.

(19) Mukherjee, J.; Yang, Z. Y.; Lew, R. *N*-(6−18F-fluorohexyl)-*N*-methylpropargylamine: a fluorine-18-labeled monoamine oxidase B inhibitor for potential use in PET studies. *Nucl. Med. Biol.* **1999**, *26*, 111–116.

(20) Plenevaux, A.; Fowler, J. S.; Dewey, S. L.; Wolf, A. P.; Guillaume, M. The synthesis of no-carrier-added DL-4-[18F]fluorodeprenyl via the nucleophilic aromatic substitution reaction. *Int. J. Rad. Appl. Instrum., A* **1991**, *42*, 121–127.

(21) Bowen, R. D.; Harrison, A. G.; Reiner, E. J. Ion−dipole complexes in the unimolecular reactions of isolated organic ions-effect of *N*-methylation on olefin and amine loss from protected aliphatic-amines. *J. Chem. Soc., Perkin Trans. 2* **1988**, 1009–1013.

(22) Couty, F.; Durrat, F.; Prim, D. Expeditive synthesis of homochiral fused tri- and tetrazoles-piperazines from beta-amino alcohols. *Tetrahedron Lett.* **2004**, *45*, 3725–3728.

(23) Metro, T. X.; Appenzeller, J.; Pardo, D. G.; Cossy, J. Highly enantioselective synthesis of beta-amino alcohols. *Org. Lett.* **2006**, *8*, 3509–3512.

(24) Weissbach, H.; Smith, T. E.; Daly, J. W.; Witkop, B.; Udenfriend, S. A rapid spectrophotometric assay of mono-amine oxidase based on the rate of disappearance of kynuramine. *J. Biol. Chem.* **1960**, *235*, 1160–1163.

(25) Hall, H.; Halldin, C.; Farde, L.; Sedvall, G. Whole hemisphere autoradiography of the postmortem human brain. *Nucl. Med. Biol.* **1998**, *25*, 715–719.

(26) Schou, M.; Halldin, C.; Pike, V. W.; Mozley, P. D.; Dobson, D.; Innis, R. B.; Farde, L.; Hall, H. Post-mortem human brain autoradiography of the norepinephrine transporter using (*S*,*S*)-[18F]FMeNER-D2. *Eur. Neuropsychopharmacol.* **2005**, *15*, 517–520.

(27) Gillberg, P. G.; Jossan, S. S.; Askmark, H.; Aquilonius, S. M. Large section cryomicrotomy for invitro receptor autography. *J. Pharmacol. Methods* **1986**, *15*, 169–180.

(28) Gulyas, B.; Makkai, B.; Kasa, P.; Gulya, K.; Bakota, L.; Varszegi, S.; Beliczai, Z.; Andersson, J.; Csiba, L.; Thiele, A.; Dyrks, T.; Suhara, T.; Suzuki, K.; Higuchi, M.; Halldin, C. A comparative autoradiography study in post mortem whole hemisphere human brain slices taken from Alzheimer patients and age-matched controls using two radiolabelled DAA1106 analogues with high affinity to the peripheral benzodiazepine receptor (PBR) system. *Neurochem. Int.* **2009**, *54*, 28–36.

■ NOTE ADDED AFTER ASAP PUBLICATION

This paper was published on the Web on September 19, 2011 without the required corrections. The corrected version was reposted on October 20, 2011.